ACS OMEGA

Open Access

http://pubs.acs.org/journal/acsodf

Review

Conformational Enigma of TDP-43 Misfolding in Neurodegenerative Disorders

Published as part of ACS Omega special issue "Celebrating the 25th Anniversary of the Chemical Research Society of India".

Meenakshi Pillai and Santosh Kumar Jha*

Cite This: *ACS Omega* 2024, 9, 40286−40297

Read Online

ACCESS | Metrics & More | Article Recommendations

ABSTRACT: Misfolding and aggregation of the protein remain some of the most common phenomena observed in neurodegeneration. While there exist multiple neurodegenerative disorders characterized by accumulation of distinct proteins, what remains particularly interesting is the ability of these proteins to undergo a conformational change to form aggregates. TDP-43 is one such nucleic acid binding protein whose misfolding is associated with many neurogenerative diseases including amyotrophic lateral sclerosis (ALS) and fronto-temporal lobar degeneration (FTLD). TDP-43 protein assumes several different conformations and oligomeric states under the diseased condition. In this review, we explore the intrinsic relationship between the conformational variability of TDP-43 protein, with a particular focus on the RRM domains, and its propensity to undergo aggregation. We further emphasize the probable mechanism behind the formation of these conformations and suggest a potential diagnostic and therapeutic strategy in the context of these conformational states of the protein.

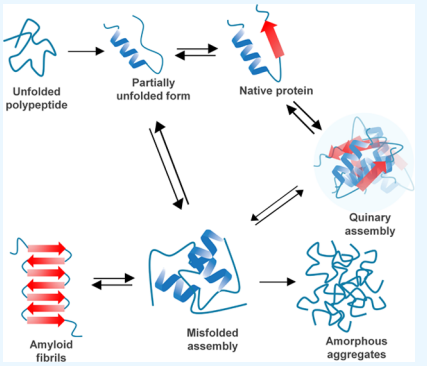

NEURODEGENERATION AND PROTEIN AGGREGATION

All cells, including neurons, experience death. In particular, neurodegeneration involves a gradual loss of specific neurons, which coincides with the clinical syndromes witnessed typically in a rapidly aging population. Neurodegeneration is an umbrella term used to define a variety of diseases, some of which include Alzheimer's disease (AD),[1,2] Parkinson's disease (PD),[3] Huntington's disease (HD),[4] Guam-Parkinsonism,[5] amyotrophic lateral sclerosis (ALS),[6] and fronto-temporal lobar degeneration (FTLD).[7] Each of these distinct diseases involves the deposition or aggregation of distinct proteins in different anatomical regions of the brain, often reflecting the symptoms of the diseases. For example, in AD, we observe major deposition of Aβ and tau protein in the medial temporal lobe and neocortical structures, and nonfunctionality of this region results in cognitive impairment, including memory loss, difficulty in reading and writing, loss of impulse control, etc.[8,9] In contrast, for ALS, the deposition of the TAR DNA binding protein is primarily seen in the upper and lower motor neurons. The degeneration of the upper motor neuron gives rise to hyper-excitability and spasticity, while the degeneration of the lower motor neuron results in muscle weakness, fasciculation, and muscular atrophy, etc.[10] Among the causative factors that have been consistently observed in neurodegenerative diseases are chronic environmental stress, deposition of protein aggregates, and inefficient clearance of the protein aggregates from the cell due to dysfunctional ubiquitin-proteasome system, nonfunctional autophagosomal/lysosomal system, excitotoxic insult, synaptic failure, mitochondrial dysfunction, and neuroinflammation.[11] Compelling evidence suggests that oligomerization of the proteins leading to the deposition of amyloids is the fundamental cause of neuronal loss and degeneration.[12,13] Different diseases show deposition of different proteins such as Aβ and tau in Alzheimer's, α-synuclein in Parkinson's, polyglutamine protein in Huntington's disease, and TDP-43 in ALS and FTLD. Despite the differences in their primary sequence and overall structural fold of the soluble precursor protein, the aggregates are characterized by highly ordered cross-β sheet rich structure.[14,15] Therefore, there appears to be a common underlying mechanism that might populate generic conformational states along the energy landscape of aggregation-prone

Received: April 29, 2024
Revised: August 25, 2024
Accepted: September 5, 2024
Published: September 20, 2024

proteins. Characterization of these conformational states and understanding the kinetic barriers between them could shed light on new avenues to detect and target pathological protein.

In this review, we discuss how alterations in local environmental conditions influence the conformational plasticity of proteins in general, mainly examining this phenomenon through the lens of energy landscape. Our discussion centers on the TDP-43 protein with a particular focus on understanding the role of RRM domains in aggregation and lists out the potential mechanisms involved behind the formation of different conformational states for TDP-43 protein.

TDP-43 IS A MAJOR PROTEIN AGGREGATE IN ALS AND FTLD

The gene coding for TAR DNA binding protein is well conserved among Drosophila, human, mouse, and *Caenorhabditis elegans*.[16] The 43 kDa protein, TDP-43, was first discovered in 1996 for its role in binding to the TAR DNA of HIV and repressing the transcription process.[17] TDP-43 was later studied for its role as an exon-skipping promoter during the splicing of apolipoprotein A-II (apoA-II) and cystic fibrosis transmembrane regulator (CFTR) transcripts. Despite its various vital functions, TDP-43 protein was found to be a major protein deposited in the spinal cord and brain of patients suffering from ALS and FTLD.[18,19] Since then, several neurodegenerative diseases such as Alzheimer's, Parkinson's, Huntington's, Guam-Parkinsonism dementia, and Perry's syndrome have shown intraneuronal deposition of TDP-43 aggregates.[20−23] More recently, limbic-predominant age-related TDP-43 encephalopathy-neuropathological change (LATE-NC) was recognized as a brain disorder affecting older adults showing accumulation of TDP-43.[24] Together, these diseases showing deposition of TDP-43 protein were termed TDP-43 proteinopathies.[25]

TDP-43 IS A NUCLEIC ACID BINDING PROTEIN WITH AN INTRINSICALLY DISORDERED REGION

Structurally, TDP-43 protein has four major domains, an N-terminal domain: NTD (aa, 1−76), two RNA recognition motif domains: RRM1 (amino acids 104−176) and RRM2 (amino acids 192−262) linked via a linker region, and a C-terminal domain: CTD (aa 274−414).[26−29] The protein has two signal sequences: a nuclear localization signal (NLS; aa 82−98) and a nuclear export signal (NES; aa 239−250), through which it shuttles between the nucleus and cytoplasm to perform its function.[30] TDP-43 is primarily a nuclear protein but in the case of ALS, the protein is redistributed, showing an increased deposition in the form of inclusions in the cytoplasm.[31] Due to high aggregation propensity and poor solubility, the complete structure of TDP-43 remains unresolved until now, but the role of individual domains in aggregation is being addressed.

Experimental evidence suggests that TDP-43 protein remains in a monomer−dimer equilibrium inside the cell under normal conditions.[32,33] The process of dimerization is shown to be facilitated by the N-terminal domain of TDP-43.[34−36] It has been reasoned that the dimeric NTD enhances the solubility of the protein through its pre-mRNA splicing activity and protects against inclusion formation.[37] In contrast to this idea, studies have also suggested that dimerization may be involved in the aggregation of the protein.[32−34] These studies imply that the N-terminal region may increase the local concentration of the protein which can serve as a prerequisite for aggregation reaction.[38,39] The C-terminal domain of TDP-43 consists of a glycine-rich region and a segment containing polar uncharged amino acids, such as glutamine and asparagine (Q/N). This domain architecture is highly comparable to the prionlike domains of several proteins such as Sup35, Fused-In-Sarcoma (FUS), TATA-box binding protein associated factor 15 (TAF-15), and Ewing sarcoma breakpoint region 1 (EWSR1) and heterogeneous nuclear ribonucleoproteins (hnRNPs) family of proteins.[40] A vast number of studies in the literature focus on the contribution of the CTD toward the aggregation of the protein. A chief reason for using the C-terminal region as a model domain is because it harbors the majority of the mutations and phosphorylation sites.[41−44] A detailed review of the CTD of TDP-43 and its involvement in the diseased condition has been reviewed previously.[45,46] Additionally, it has also been seen that C-terminal fragments of sizes ∼25−35 kDa are observed in the inclusion bodies.[47,48] Cleavage of these fragments occurs at the caspase site located on the RRM2 domain of TDP-43 protein,[47] prompting us to hypothesize that partial unfolding of the RRM domain might also be pivotal in the aggregation process.

ROLE OF RRM DOMAINS OF TDP-43 IN FUNCTION AND AGGREGATION

RRM is a Well-Folded Nucleic-Acid Binding Domain. RNA recognition motifs present in the RNA binding proteins (RBPs) are among the most abundant and conserved domains in the eukaryotes.[49−51] The RRM domains of TDP-43 contain a conserved set of amino acids that bind to nucleic acids and perform a host of different functions such as mRNA transcription and splicing, mRNA transport, mRNA maturation and stability, and mRNA translation.[52−55] TDP-43 has two RRM domains separated by 15 amino acid residue linker, folded into 5 β-stranded sheets and 2 α-helices arranged in a $\beta1$-$\alpha1$-$\beta2$-$\beta3$-$\alpha2$-$\beta4$-$\beta5$ pattern.[26] Unlike the typical 4 strands present in an RRM domain,[55] there is an additional β strand present in TDP-43, which is believed to give stability to the protein.[56] The two RRM domains can bind to UG- and TG-rich sequences.[26,27] RRM1 binds to UG_6 with a K_d of 65.2 nM while RRM2 binds to UG_3 with a K_d of 379 nM. RRM1 contains a longer loop3 region as compared to RRM2, which is believed to contribute to RRM1's higher affinity for nucleic acid interaction.[57] However, when both the RRM domains bind to UG_6, there is a synergistic binding effect that drastically increases binding affinity and reduces the K_d to 14.2 nM.[27] Interestingly, the TDP-43 RRM domains bind to RNA in a reverse manner, unlike the typical RRM domains that usually bind in a 3′-to-5′ direction.[26] This reverse interaction allows the 15 residue linker to participate more extensively with the nucleic acid targets.[26] Apart from playing an important role in function, binding to nucleic acid has also been shown to rescue the protein from undergoing aggregation.[58−60]

CONFORMATIONAL CHANGES WITHIN THE RRM DOMAINS OF TDP-43 DURING STRESS CONDITIONS: FORMATION OF OLIGOMER WITH MOLTEN GLOBULELIKE STRUCTURE

An NMR study, coupled with X-ray fiber diffraction data, highlights a strong similarity in the structure of amyloid fibrils formed by full-length TDP-43 and TDP-35 (90−414 residue).[61] The C-terminus showed a polymorphic structure

https://doi.org/10.1021/acsomega.4c04119
ACS Omega 2024, 9, 40286−40297

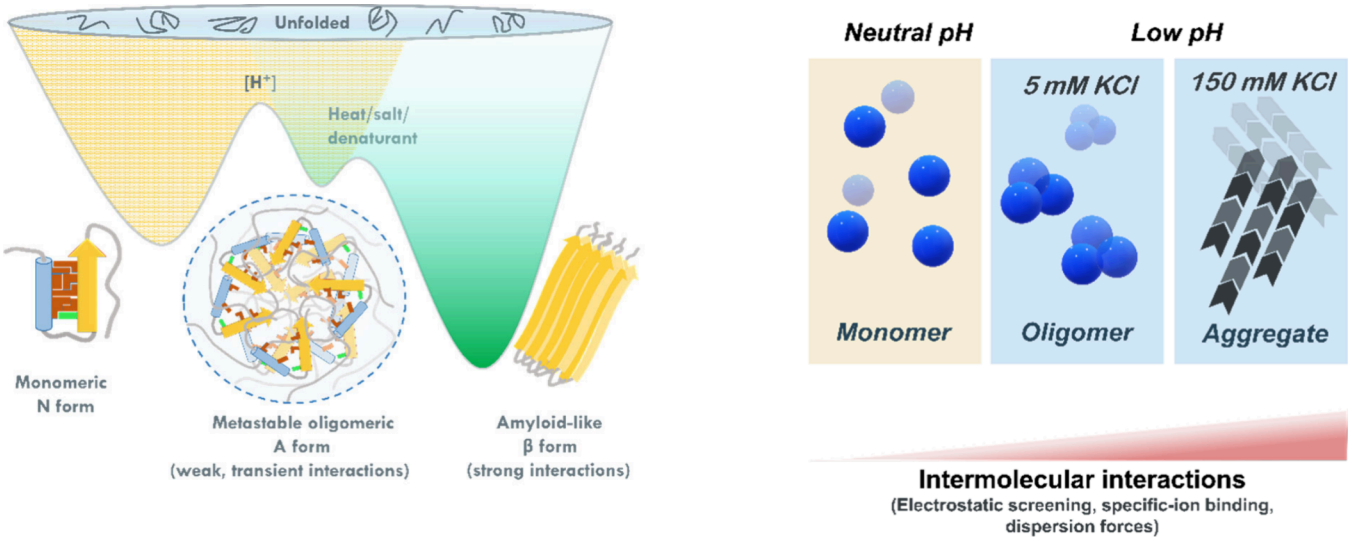

Figure 1. Formation of metastable, molten-globulelike oligomers that bridges the folding and aggregation energy landscapes. Reproduced from ref 63. Copyright 2019 American Chemical Society. The cartoon on the right represents the conformational changes in the RRM domains of TDP-43 driven by altered electrostatics. Reproduced from ref 68. Copyright 2023 American Chemical Society.

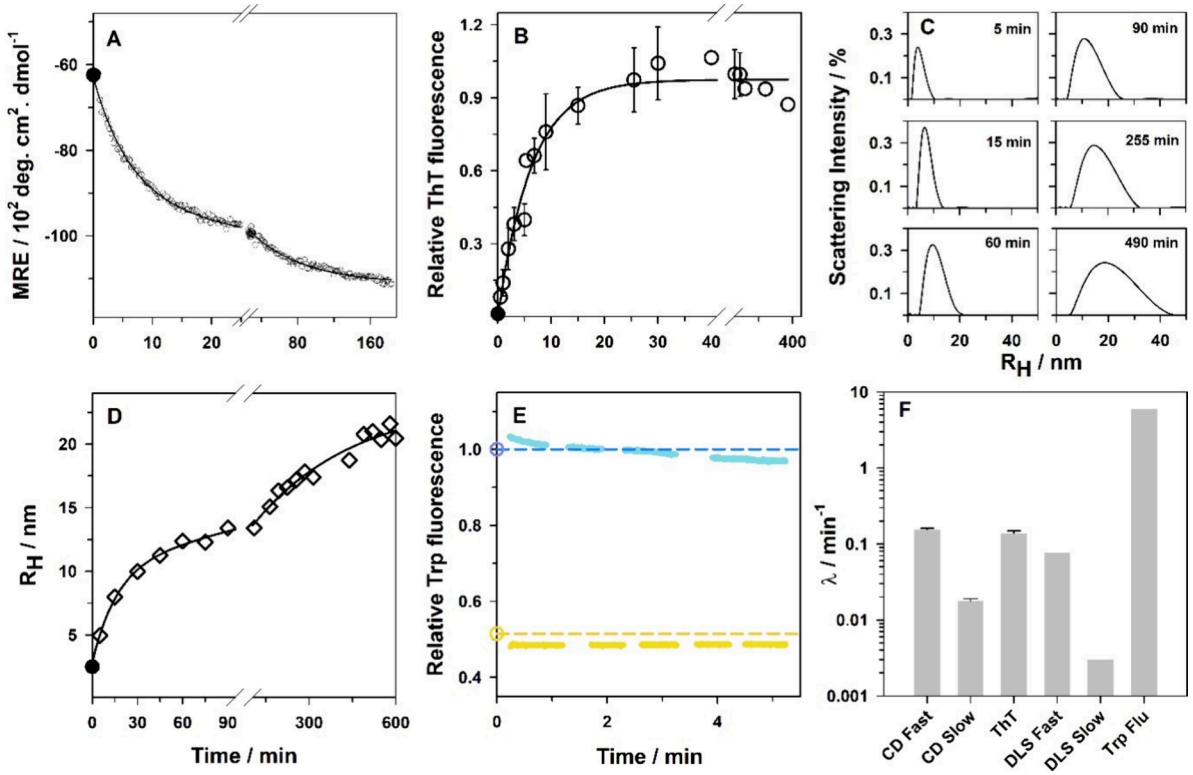

Figure 2. RRM domains of TDP-43 undergo a multistep structural transformation upon protonation of a buried ionizable residue, leading to the formation of a fibrillar structure. The kinetic data presented here monitors the time scales of different structural conformations during the aggregation process. (A) Changes in the protein's secondary structure, monitored through far-UV circular dichroism. (B) Formation of ThT-binding pockets. (C and D) Increase in protein assembly size as tracked by dynamic light scattering. (E) Changes in the local tertiary structure, observed via tryptophan fluorescence for the protein before (blue line) and after (yellow line) transfer into aggregation buffer. Data from these panels were analyzed using single or double exponential equations, and (F) the apparent rate constants derived from these fits. The black-filled circles in panels A, B, and D indicate signal of the protein before transferring into the aggregation condition. Adapted with permission from ref 67. Copyright 2023 John Wiley and Sons.

when forming fibrils alone or in combination with other domains. This suggests that both the N-terminal and RRM domains are crucial in forming the core structure of TDP-43.[61] The RRM domains of TDP-43 have been studied individually[62] and in tandem[63,64] and shown to undergo aggregation. Two regions within the RRM domains have been identified to play a vital role in the aggregation process: residues 166−173 in RRM1 and residues 246−255 in RRM2.[56,65]

Studies from our lab showed that protonation of residue H166 causes destabilization of the RRM domains causing it to

https://doi.org/10.1021/acsomega.4c04119
ACS Omega 2024, 9, 40286−40297

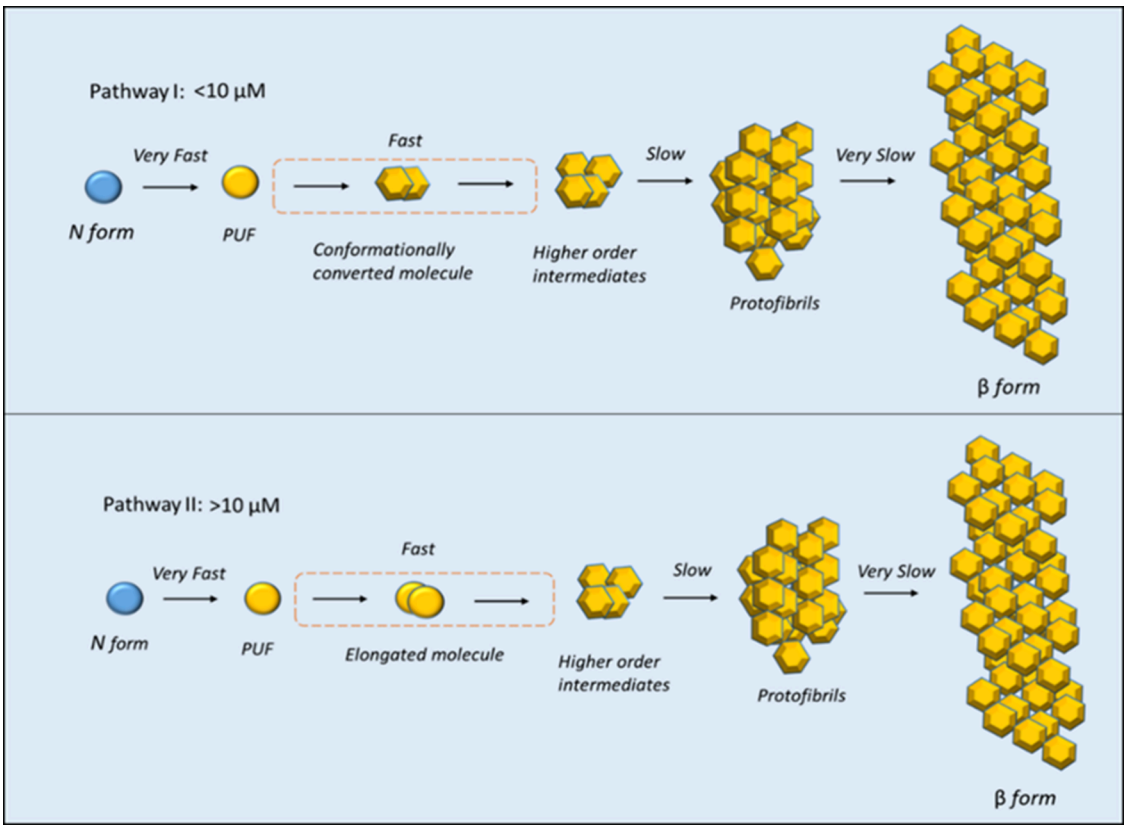

Figure 3. Multistep model for the aggregation of the RRM domains of TDP-43. This kinetic model is built using the apparent rate constants obtained from Figure 2. The model illustrates how the protein concentration influences the rate-limiting step in the aggregation process. It depicts four major stages in the aggregation process, each corresponding to a distinct change in the conformation and size of the protein assembly over time. Adapted with permission from ref 67. Copyright 2023 John Wiley and Sons.

partially unfold and result in the formation of nativelike oligomers with an intact secondary structure and a broken tertiary structure (molten globule).[63,64,66] Thus, the protonation−deprotonation of His166 residue regulates the assembly disassembly of protein molecules (Figure 1).[63,66] Upon prolonged stress, these oligomers can undergo a conformational change to form ThT-positive aggregates, thus acting as a bridge to link the native and the aggregation energy landscape (Figure 1).[67] Our time-dependent analysis of the aggregation process uncovered a multistep structural transformation (Figure 2), which we have modeled to reveal four major steps, each characterized by varying energy barriers. The sequence of these steps depends on the protein concentration (Figures 2 and 3).[67] Our data suggest that the initial partial unfolding, triggered by side-chain disruption from protonation, is sufficient to overcome the major energy barrier and drive the protein through a series of conformational changes following a linear (isodesmic) polymerization mechanism (Figure 3).[67] Consequently, the population and stability of the different states of protein (monomer, oligomer, or aggregates) were shown to be highly dependent on the intramolecular and intermolecular interactions, which are modulated by changing the electrostatic conditions through pH and salt in the solution (Figure 1).[68,69] Several in vitro studies have demonstrated that a change in the pH destabilizes the protein molecules and induces a conformational change to form aggregates under prolonged stress conditions.[64,70−73] In some proteins, protonation has been shown to act as a molecular switch controlling the equilibrium between native and the partially unfolded molecules that can prime misfolded structures.[64,66,74−76] Consistent with this idea, it has been shown that assembly disassembly is one of the most energy-efficient ways to mitigate stress, unlike post-translational modification or degradation.[77] Additionally, the time scales of formation of these higher-order assemblies are also less, allowing the cells to quickly respond to stress-like conditions.[77] Formation of such molten globule states were also observed for other neurodegenerative proteins such as β2-microglobulin (β2m),[78,79] prion,[80] and p53.[81,82]

Electrostatics in the cell are often altered either by post-translational modification of side chains or by the presence of mutations in the protein. For example, two crucial electrostatic mutations are present within RRM domains, P112H and D169G.[83,84] The mutation D169G in the RRM1 domain does not affect the aggregation propensity but induces a local conformational change due to the loss of hydrogen bond with T115 residue.[85] We also demonstrated that these mutants do not alter the global structure of the tandem RRM domains. However, under pH and salt stress, the aggregation kinetics of P112H increases significantly as compared to the wild-type sequence, while D169G remains largely comparable to the wild-type sequence. Under oxidation stress or upon binding to zinc ions, these domains undergo oligomerization or formation of ThT-positive aggregates.[86−88] Structural studies have also revealed that the RRM2 domain of TDP-43 populates an intermediate state that has been proposed to act as a link between the folding and the misfolding energy landscape.[89] All these studies reinforce the notion that destabilization of RRM domains through changes in protonation, oxidation, or zinc-

https://doi.org/10.1021/acsomega.4c04119
ACS Omega 2024, 9, 40286−40297

binding can induce partial unfolding and expose hydrophobic patches in the protein, leading to aggregate formation. Conversely, stabilization of protein through RNA/DNA binding has been shown to mitigate the process of aggregation.[58,59,66]

RRM domains, in general, contribute to the architecture of many aggregation-prone proteins such as FUS, hnRNPs, TAF-15, and EWSR1, which are associated with various neurodegenerative diseases.[40,90] Remarkably, around ∼240 proteins within the human proteome contain prionlike low complexity domain, many of which also harbor a canonical RNA Recognition Motif.[10,91] Numerous studies have focused on the role of low complexity domain in misfolding and aggregation, but investigations with emphasis on the role of RRM domain in aggregation is only now evolving.[92]

CONFORMATIONAL VARIABILITY IN THE AGGREGATES FROM BRAIN PATIENTS

TDP-43 Oligomers: Evidence from Invitro and Patient Studies. A prevailing hypothesis for the involvement of pathogenic proteins in neurodegenerative diseases is the presence of oligomers and aggregates that cause the protein to lose its normal function (loss of function) and cause neurotoxicity (gain of function).[93,94] Evidence supporting this hypothesis has been demonstrated by the presence of TDP-43 oligomers that exhibited lower DNA binding activity and appeared structurally different from the native TDP-43.[95] These oligomers have been shown to bind to oligomer-specific A11 antibody that has previously been shown to interact with oligomers of Aβ, tau, and α-synuclein proteins, suggesting that TDP-43 oligomers share a common structural homology with other amyloids.[95,96] Treatment with arsenite, a commonly used stress-inducing agent in human neuroblastoma SH-SY5Y cells, caused a liquid-to-gel like transition that was positive for A11 antibody.[97] The occurrence of TDP-43 oligomers among the FTLD-TDP patients was further validated by the development of a polyclonal TDP-43 oligomer antibody, known as TDP-O, thus confirming their presence.[98] A study using an induced pluripotent stem cell (iPSC) model found that recombinant TDP-43 oligomers can also induce neuronal toxicity.[99] Together, these studies establish the presence of a wide spectrum of TDP-43 oligomers ranging from dimers, trimers, and tetramers to higher molecular weight species, underscoring their significant role in pathology.

TDP-43 As a Part of the Multimeric Structure: Stress Granules, Nuclear Bodies, Anisosomes, and Amorphous Inclusions. TDP-43 forms a major component of several membraneless organelles, such as stress granules and nuclear paraspeckles. Research has explored the critical role played by all three domains of TDP-43. The NTD was shown to be responsible for head-to-tail polymerization, while interactions between helices of the LCD stabilized the LLPS.[35] Furthermore, binding to RNA through the RRM domain also promoted liquid-like granule formation in cells.[100] RRM plays a crucial role in the formation of nuclear bodies (NB) in cells. The two RRM domains were shown to respond to different RNA acting distinctly in the assembly of NBs.[100] In an RNA-binding deficient TDP-43, the protein was shown to undergo a distinct type of LLPS with chaperones assembling into a dynamic spherical shell-like structure called anisosomes.[101] Furthermore, the ablation of RNA-binding or acetylation-mimicking TDP-43 modification led to the depletion of nuclear TDP-43 and enhanced the aggregation propensity by directly affecting the solubility and mobility dynamics of TDP-43 protein.[102] Upon inducing phase separation of the full-length TDP-43 protein, it formed assemblies with limited internal diffusion.[103] Instead of exhibiting typical liquid−liquid phase separation (LLPS) behavior such as coalescing, the protein formed irregular assemblies.[103] This contrasts with the characteristic LLPS behavior observed with CTD from many independent groups.[43,44,104,105]

One of the most prevalent hypotheses in the field is that the stress granules (SG) formed in response to cellular stress might fail to disassemble, leading to inclusion formation in the diseased condition. Factors that affect the residence time of the protein in SG might be influenced by post-translational modification, pathological mutation in the protein, or depletion of cellular ATP.[106−109] However, it remains unclear how the dynamicity of the reversible SG assembly converts into a more mature amyloid or amorphous aggregate. For TDP-43, multiple studies have shown that a subset of TDP-43 contains cytoplasmic inclusions that labels for SG markers such as TIA1, eIF3, PABP, and HuR.[110−115] It would be interesting to study how the different SGs containing TDP-43 alter the dynamicity of the protein. Further literature on the relationship between TDP-43 and stress granules can be found in previously published reviews.[45,116,117]

POLYMORPHISM IN THE AMYLOID FOLD OF THE AGGREGATES

Under diseased conditions, both full-length TDP-43 and truncated C-terminal fragments (CTFs) form granulo-filamentous assemblies with diameters of 10−15 nm.[118−121] Cryo-EM structures from two individuals suffering from ALS with FTLD degeneration (type B) revealed an identical double-spiral-shaped fold, distinct from those observed using recombinant TDP-43 invitro.[122−124] This ordered core was formed by the fragment (G282−Q360) with flanking regions forming a fuzzy coat. In contrast, TDP-43 assemblies from type A FTLD-TDP individuals exhibited a distinct extended structural fold resembling a chevron.[125] Although the same region contributed to the formation of the ordered core, the authors hypothesized that the local structural variations within individual filaments might give rise to alternative conformations. These structural differences may explain the distinct pathologies observed in different types of FTLD-TDP, which are characterized by the brain distribution of aggregated TDP-43.[125] The different local environmental conditions might likely influence the conformation, giving rise to distinct amyloid-fold.

Under in vitro conditions, different environmental conditions such as pH, temperature, mechanical agitation, or ionic strength give rise to different assemblies.[126,127] However, once a scaffold is formed, the growth continues, keeping the atomistic order the same, even when the solution condition is changed. A specific polymorph can seed the same type of architecture even under different solution conditions, similar to those observed in crystalline systems.[128] This has been studied in the case of Aβ_{40}, where the formation of striated ribbons and twisted fibrils formed under agitation and quiescent conditions, respectively, when used to act as a seed, propagated similar structures under different conditions.[129] This might be due to the intrinsic stability of the extremely ordered architecture and the high energy barriers between the different polymorphs.

https://doi.org/10.1021/acsomega.4c04119
ACS Omega 2024, 9, 40286−40297

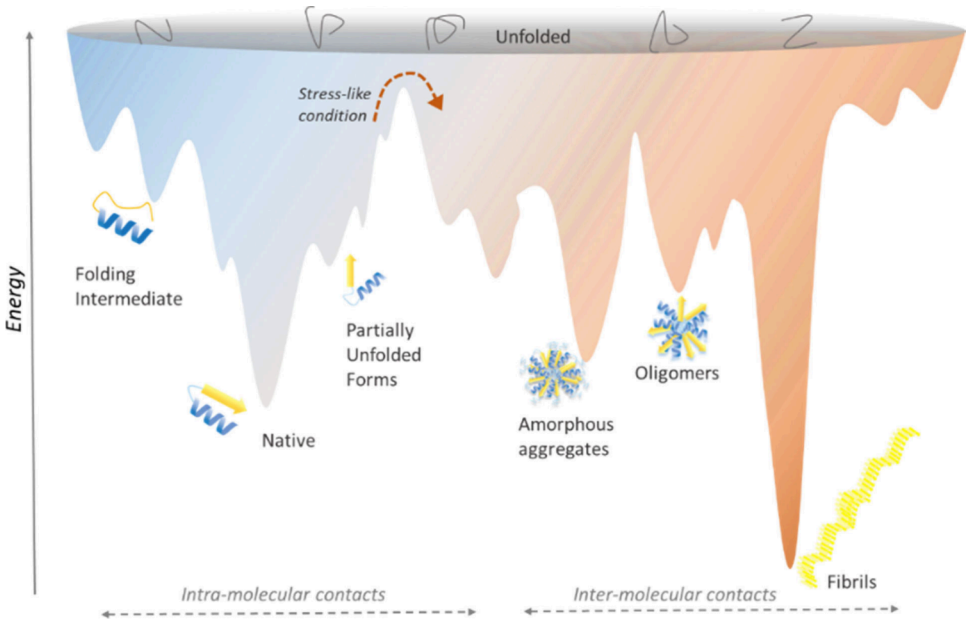

Figure 4. Folding energy landscape indicates the search for a polypeptide to achieve its native state. The aggregation energy landscape illustrated by the dark brown color represents the different kinds of intermediates and assembly formation under stresslike conditions. The various energy minima on the landscape represents the possibility of formation of different intermediates and their respective stability.

In general, polymorphism seen in the amyloid can be attributed to the side-chain conformation, backbone conformation, or supramolecular assembly. Several different proteins such as Aβ40,[130−133] α-synuclein,[134−136] islet amyloid polypeptide (IAPP),[137] tau,[138,139] and prion[140] show polymorphic amyloid fibrils. A range of different conformations adopted by the protein can often contribute distinctly to its toxicity and transmission.[141,142] Unlike a native fold which is evolutionarily selected, the formation of an amyloid fold is not optimized by evolutionary pressure, and hence, there is a multitude of different arrangements that becomes accessible to the polypeptide sequence.[128]

MODULATION OF THE ENERGY LANDSCAPE: TARGETING THE NATIVE STATE, INTERMEDIATE, AND THE AGGREGATED STATES OF THE PROTEIN

The energy landscape concept illustrates the conformational space available for a polypeptide sequence to form a structure, resembling a funnel where the ruggedness depends on various factors (Figure 4).[143,144] In a complex microenvironment, the energy landscape will typically be rough for a multifunctional protein, which can often be correlated to frustration in the folding process.[145] Experimental evidence suggests that for a well-folded globular protein to undergo the formation of amyloid or amorphous aggregates, it requires partial unfolding and destabilization of its native structure (Figure 4).[12,13,146−150] Many aggregation-prone proteins show the formation of partially unfolded structures under destabilizing conditions such as β2 microglobulin,[76] prion,[151,152] superoxide dismutase 1 (SOD1),[153] and transthyretin (TTR).[154] Transient formations of such partially unfolded species allow specific electrostatic, hydrophobic, and intermolecular interactions that enable the protein to undertake key structural rearrangements to undergo fibril formation.[147]

Given that the structural conformations formed early during the aggregation process are often reversible, targeting these conformations by stabilizing them and driving the equilibrium away from higher-order aggregates offers an opportunity to develop therapeutic modulators (Figure 5). For example,

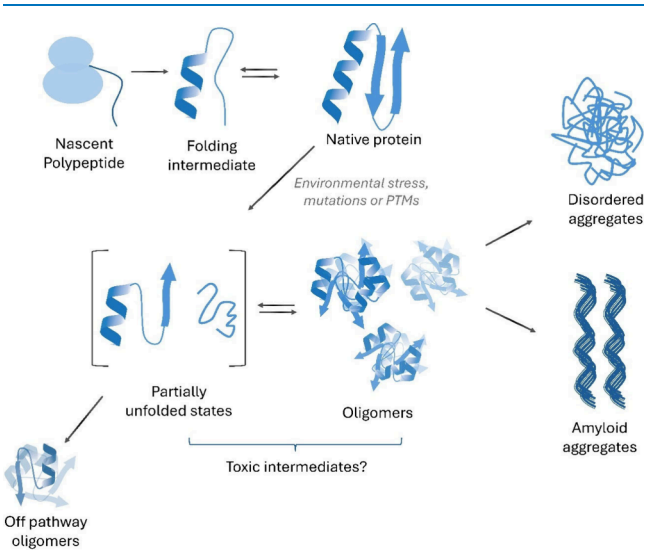

Figure 5. Complex multistep aggregation process and the heterogeneity observed during the aggregation reaction. The pathway illustrates the formation of different intermediates, both on-pathway and off-pathway, as well as generation of different assemblies, including oligomers. Potential therapeutic strategies include stabilizing the native state, diverting the reaction to off-pathway intermediates, or developing small molecules that bind to the aggregates.

tafamidis is a small molecule kinetic stabilizer that stabilizes the native tetrameric state of TTR and is FDA-approved for TTR amyloidosis.[155] Similar kinetic stabilizers are being developed to stabilize the native dimer of the immunoglobulin light chain, which can form aggregation-prone conformations in the immunoglobulin light chain amyloidosis.[156] Native state stabilization as a therapeutic strategy has more recently been

https://doi.org/10.1021/acsomega.4c04119
ACS Omega 2024, 9, 40286−40297

adapted for treating TDP-43 proteinopathies. Leveraging Cryo-EM structures of TDP-43 fibrils, the study proposed to develop a high-throughput screening assay to identify and develop a native state stabilizer.[157] One such native state stabilizer for TDP-43 can be RNA which has been consistently reported to stabilize the protein and prevent it from undergoing aggregation.[157]

Another approach would be to target the on-pathway oligomers and intermediates during the aggregation process (Figure 5). For example, cysteine-reactive small molecules, designed from conformational motifs in dimeric and hexameric intermediates of human β2m, promote off-pathway tetramer production that inhibits aggregation.[158] Yet another approach is to directly target the aggregates formed. Along these lines, a recent study successfully utilized a molecule "baicalein", a structure-correcting agent that can convert the existing TDP-43 aggregates into a functional oligomeric state in the disease model.[159] While baicalein was shown to effectively mitigate the proteinopathies in the mouse model, it still remains to be seen if it can effectively refold the TDP-43 protein into a nonpathological conformation.[160] An interesting tactic developed by Eisenberg et al. involved designing mini proteins that could specifically target and cap the growing ends of α-synuclein, Aβ, and tau fibrils.[161] Using this approach, they were successfully able to slow down the seeded aggregation of these proteins in vitro, in human cells, and in *C. elegans* models of AD and PD.[161] Multiple studies have adapted these strategies to specifically target the fibrillar structure and slow down or inhibit the aggregation of proteins.[162−165] More detailed kinetic design principles used for guidance and development of inhibitors for fibril growth can be found in a recently published study.[166]

CONCLUSION

Given the significant variation in TDP-43 proteinopathies, characterized by diverse conformations of the protein, understanding and characterizing these different structures are crucial for developing therapeutic approaches. Potential therapeutic strategies include using natural ligands like RNA to stabilize the protein, developing small molecules to target the TDP-43 fibril core, or creating phosphomimetic substitutions. This review provides a broad perspective on the various conformational states observed for the TDP-43 protein. By utilizing the framework of the energy landscape, we explore how targeting these key structures could open new avenues for treating these diseases.

AUTHOR INFORMATION

Corresponding Author

Santosh Kumar Jha − *Physical and Materials Chemistry Division, CSIR-National Chemical Laboratory, Pune 411008, India; Academy of Scientific and Innovative Research (AcSIR), Ghaziabad 201002, India;* orcid.org/0000-0003-1339-7409; Phone: 91-20-25902588; Email: sk.jha@ncl.res.in; Fax: 91-20-25902615

Author

Meenakshi Pillai − *Physical and Materials Chemistry Division, CSIR-National Chemical Laboratory, Pune 411008, India; Academy of Scientific and Innovative Research (AcSIR), Ghaziabad 201002, India;* Present Address: Johns Hopkins University, Baltimore, Maryland 21205, United States

Complete contact information is available at: https://pubs.acs.org/10.1021/acsomega.4c04119

Notes

The authors declare no competing financial interest.

ACKNOWLEDGMENTS

This work was funded by a SERB-DST core research grant (project CRG/2023/002721) to S.K.J. M.P. received a Senior Research Fellowship from the University Grants Commission, India.

REFERENCES

(1) Selkoe, D. J. The molecular pathology of alzheimer's disease. *Neuron* **1991**, *6*, 487−98.
(2) Hardy, J. The Alzheimer family of diseases: Many etiologies, one pathogenesis? *Proc. Natl. Acad. Sci. U. S. A.* **1997**, *94*, 2095−2097.
(3) Poewe, W.; Seppi, K.; Tanner, C. M.; Halliday, G. M.; Brundin, P.; Volkmann, J.; Schrag, A. E.; Lang, A. E. Parkinson disease. *Nat. Rev. Dis. Primers* **2017**, *3*, 17013.
(4) Walker, F. O. Huntington's disease. *Lancet* **2007**, *369*, 218−28.
(5) Steele, J. C. Parkinsonism-dementia complex of guam. *Mov. Disord.* **2005**, *20*, S99−S107.
(6) Rowland, L. P.; Shneider, N. A. Amyotrophic lateral sclerosis. *N. Engl. J. Med.* **2001**, *344*, 1688−1700.
(7) Seltman, R. E.; Matthews, B. R. Frontotemporal lobar degeneration: Epidemiology, pathology, diagnosis and management. *CNS Drugs* **2012**, *26*, 841−70.
(8) Breijyeh, Z.; Karaman, R. Comprehensive review on alzheimer's disease: Causes and treatment. *Molecules* **2020**, *25*, 5789.
(9) De-Paula, V. J.; Radanovic, M.; Diniz, B. S.; Forlenza, O. V. Alzheimer's disease. *Subcell Biochem* **2012**, *65*, 329−352.
(10) Prasad, A.; Bharathi, V.; Sivalingam, V.; Girdhar, A.; Patel, B. K. Molecular mechanisms of TDP-43 misfolding and pathology in amyotrophic lateral sclerosis. *Front. Mol. Neurosci.* **2019**, *12*, No. 25.
(11) Bossy-Wetzel, E.; Schwarzenbacher, R.; Lipton, S. A. Molecular pathways to neurodegeneration. *Nat. Med.* **2004**, *10*, S2−9.
(12) Kelly, J. W. The alternative conformations of amyloidogenic proteins and their multi-step assembly pathways. *Curr. Opin. Struct. Biol.* **1998**, *8*, 101−106.
(13) Dobson, C. M. The structural basis of protein folding and its links with human disease. *Philos. Trans R Soc. Lond B Biol. Sci.* **2001**, *356*, 133−145.
(14) Sunde, M.; Blake, C. The structure of amyloid fibrils by electron microscopy and X-ray diffraction. *Adv. Protein Chem.* **1997**, *50*, 123−59.
(15) Makin, O. S.; Serpell, L. C. Examining the structure of the mature amyloid fibril. *Biochem. Soc. Trans.* **2002**, *30*, 521−5.
(16) Wang, H. Y.; Wang, I. F.; Bose, J.; Shen, C. K. Structural diversity and functional implications of the eukaryotic TDP gene family. *Genomics* **2004**, *83*, 130−9.
(17) Ou, S. H.; Wu, F.; Harrich, D.; Garcia-Martinez, L. F.; Gaynor, R. B. Cloning and characterization of a novel cellular protein, TDP-43, that binds to human immunodeficiency virus type 1 TAR DNA sequence motifs. *J. Virol* **1995**, *69*, 3584−96.
(18) Neumann, M.; Sampathu, D. M.; Kwong, L. K.; Truax, A. C.; Micsenyi, M. C.; Chou, T. T.; Bruce, J.; Schuck, T.; Grossman, M.; Clark, C. M.; McCluskey, L. F.; Miller, B. L.; Masliah, E.; Mackenzie, I. R.; Feldman, H.; Feiden, W.; Kretzschmar, H. A.; Trojanowski, J. Q.; Lee, V. M. Ubiquitinated TDP-43 in frontotemporal lobar degeneration and amyotrophic lateral sclerosis. *Science* **2006**, *314*, 130−133.
(19) Arai, T.; Hasegawa, M.; Akiyama, H.; Ikeda, K.; Nonaka, T.; Mori, H.; Mann, D.; Tsuchiya, K.; Yoshida, M.; Hashizume, Y.; Oda, T. TDP-43 is a component of ubiquitin-positive tau-negative inclusions in frontotemporal lobar degeneration and amyotrophic lateral sclerosis. *Biochem. Biophys. Res. Commun.* **2006**, *351*, 602−611.

https://doi.org/10.1021/acsomega.4c04119
ACS Omega 2024, 9, 40286−40297

(20) Chen-Plotkin, A. S.; Lee, V. M.; Trojanowski, J. Q. TAR DNA-binding protein 43 in neurodegenerative disease. *Nat. Rev. Neurol.* **2010**, *6*, 211−220.
(21) Hasegawa, M.; Arai, T.; Akiyama, H.; Nonaka, T.; Mori, H.; Hashimoto, T.; Yamazaki, M.; Oyanagi, K. TDP-43 is deposited in the guam parkinsonism-dementia complex brains. *Brain* **2007**, *130*, 1386−1394.
(22) Higashi, S.; Iseki, E.; Yamamoto, R.; Minegishi, M.; Hino, H.; Fujisawa, K.; Togo, T.; Katsuse, O.; Uchikado, H.; Furukawa, Y.; Kosaka, K.; Arai, H. Concurrence of TDP-43, tau and α-synuclein pathology in brains of alzheimer's disease and dementia with lewy bodies. *Brain Res.* **2007**, *1184*, 284−294.
(23) Mishima, T.; Koga, S.; Lin, W. L.; Kasanuki, K.; Castanedes-Casey, M.; Wszolek, Z. K.; Oh, S. J.; Tsuboi, Y.; Dickson, D. W. Perry syndrome: A distinctive type of TDP-43 proteinopathy. *J. Neuropathol Exp Neurol* **2017**, *76*, 676−682.
(24) Nelson, P. T.; Dickson, D. W.; Trojanowski, J. Q.; Jack, C. R.; Boyle, P. A.; Arfanakis, K.; Rademakers, R.; Alafuzoff, I.; Attems, J.; Brayne, C.; Coyle-Gilchrist, I. T. S.; Chui, H. C.; Fardo, D. W.; Flanagan, M. E.; Halliday, G.; Hokkanen, S. R. K.; Hunter, S.; Jicha, G. A.; Katsumata, Y.; Kawas, C. H.; Keene, C. D.; Kovacs, G. G.; Kukull, W. A.; Levey, A. I.; Makkinejad, N.; Montine, T. J.; Murayama, S.; Murray, M. E.; Nag, S.; Rissman, R. A.; Seeley, W. W.; Sperling, R. A.; White, C. L., 3rd; Yu, L.; Schneider, J. A. Limbic-predominant age-related TDP-43 encephalopathy (late): Consensus working group report. *Brain* **2019**, *142*, 1503−1527.
(25) Gao, J.; Wang, L.; Huntley, M. L.; Perry, G.; Wang, X. Pathomechanisms of TDP-43 in neurodegeneration. *J. Neurochem.* **2018**, *146*, 7−20.
(26) Lukavsky, P. J; Daujotyte, D.; Tollervey, J. R; Ule, J.; Stuani, C.; Buratti, E.; Baralle, F. E; Damberger, F. F; Allain, F. H-T Molecular basis of UG-rich RNA recognition by the human splicing factor TDP-43. *Nat. Struct. Mol. Biol.* **2013**, *20*, 1443−1449.
(27) Kuo, P. H.; Doudeva, L. G.; Wang, Y. T.; Shen, C. K. J.; Yuan, H. S. Structural insights into TDP-43 in nucleic-acid binding and domain interactions. *Nucleic Acids Res.* **2009**, *37*, 1799−1808.
(28) Qin, H. N.; Lim, L. Z.; Wei, Y. Y.; Song, J. X. TDP-43 N terminus encodes a novel ubiquitin-like fold and its unfolded form in equilibrium that can be shifted by binding to ssDNA. *Proc. Natl. Acad. Sci. U.S.A.* **2014**, *111*, 18619−18624.
(29) Mompean, M.; Romano, V.; Pantoja-Uceda, D.; Stuani, C.; Baralle, F. E.; Buratti, E.; Laurents, D. V. The TDP-43 N-terminal domain structure at high resolution. *FEBS J.* **2016**, *283*, 1242−60.
(30) Ayala, Y. M.; Zago, P.; D'Ambrogio, A.; Xu, Y. F.; Petrucelli, L.; Buratti, E.; Baralle, F. E. Structural determinants of the cellular localization and shuttling of TDP-43. *J. Cell Sci.* **2008**, *121*, 3778−3785.
(31) Winton, M. J.; Igaz, L. M.; Wong, M. M.; Kwong, L. K.; Trojanowski, J. Q.; Lee, V. M. Disturbance of nuclear and cytoplasmic TAR DNA-binding protein (TDP-43) induces disease-like redistribution, sequestration, and aggregate formation. *J. Biol. Chem.* **2008**, *283*, 13302−9.
(32) Shiina, Y.; Arima, K.; Tabunoki, H.; Satoh, J. TDP-43 dimerizes in human cells in culture. *Cell. Mol. Neurobiol.* **2010**, *30*, 641−652.
(33) Zhang, Y. J.; Caulfield, T.; Xu, Y. F.; Gendron, T. F.; Hubbard, J.; Stetler, C.; Sasaguri, H.; Whitelaw, E. C.; Cai, S.; Lee, W. C.; Petrucelli, L. The dual functions of the extreme N-terminus of TDP-43 in regulating its biological activity and inclusion formation. *Hum. Mol. Genet.* **2013**, *22*, 3112−22.
(34) Afroz, T.; Hock, E. M.; Ernst, P.; Foglieni, C.; Jambeau, M.; Gilhespy, L. A. B.; Laferriere, F.; Maniecka, Z.; Pluckthun, A.; Mittl, P.; Paganetti, P.; Allain, F. H. T.; Polymenidou, M. Functional and dynamic polymerization of the ALS-linked protein TDP-43 antagonizes its pathologic aggregation. *Nat. Commun.* **2017**, *8*, 45.
(35) Wang, A.; Conicella, A. E.; Schmidt, H. B.; Martin, E. W.; Rhoads, S. N.; Reeb, A. N.; Nourse, A.; Ramirez Montero, D.; Ryan, V. H.; Rohatgi, R.; Shewmaker, F.; Naik, M. T.; Mittag, T.; Ayala, Y. M.; Fawzi, N. L. A single N-terminal phosphomimic disrupts TDP-43 polymerization, phase separation, and RNA splicing. *EMBO J.* **2018**, *37*, No. e97452.
(36) Vivoli-Vega, M.; Guri, P.; Chiti, F.; Bemporad, F. Insight into the folding and dimerization mechanisms of the N-terminal domain from human TDP-43. *Int. J. Mol. Sci.* **2020**, *21*, 6259.
(37) Jiang, L. L.; Xue, W.; Hong, J. Y.; Zhang, J. T.; Li, M. J.; Yu, S. N.; He, J. H.; Hu, H. Y. The N-terminal dimerization is required for TDP-43 splicing activity. *Sci. Rep.* **2017**, *7*, 6196.
(38) Sun, Y. L.; Chakrabartty, A. Phase to phase with TDP-43. *Biochemistry* **2017**, *56*, 809−823.
(39) Carter, G. C.; Hsiung, C. H.; Simpson, L.; Yang, H.; Zhang, X. N-terminal domain of TDP43 enhances liquid-liquid phase separation of globular proteins. *J. Mol. Biol.* **2021**, *433*, 166948.
(40) King, O. D.; Gitler, A. D.; Shorter, J. The tip of the iceberg: RNA-binding proteins with prion-like domains in neurodegenerative disease. *Brain Res.* **2012**, *1462*, 61−80.
(41) Pesiridis, G. S.; Lee, V. M.; Trojanowski, J. Q. Mutations in TDP-43 link glycine-rich domain functions to amyotrophic lateral sclerosis. *Hum. Mol. Genet.* **2009**, *18*, R156−62.
(42) Conicella, A. E.; Zerze, G. H.; Mittal, J.; Fawzi, N. L. ALS mutations disrupt phase separation mediated by alpha-helical structure in the TDP-43 low-complexity C-terminal domain. *Structure* **2016**, *24*, 1537−1549.
(43) Conicella, A. E.; Dignon, G. L.; Zerze, G. H.; Schmidt, H. B.; D'Ordine, A. M.; Kim, Y. C.; Rohatgi, R.; Ayala, Y. M.; Mittal, J.; Fawzi, N. L. TDP-43 alpha-helical structure tunes liquid-liquid phase separation and function. *Proc. Natl. Acad. Sci. U. S. A.* **2020**, *117*, 5883−5894.
(44) Mohanty, P.; Shenoy, J.; Rizuan, A.; Mercado-Ortiz, J. F.; Fawzi, N. L.; Mittal, J. A synergy between site-specific and transient interactions drives the phase separation of a disordered, low-complexity domain. *Proc. Natl. Acad. Sci. U. S. A.* **2023**, *120*, No. e2305625120.
(45) Doke, A. A.; Jha, S. K. Shapeshifter TDP-43: Molecular mechanism of structural polymorphism, aggregation, phase separation and their modulators. *Biophys Chem.* **2023**, *295*, 106972.
(46) Carey, J. L.; Guo, L. Liquid-liquid phase separation of TDP-43 and FUS in physiology and pathology of neurodegenerative diseases. *Front Mol. Biosci* **2022**, *9*, 826719.
(47) Zhang, Y. J.; Xu, Y. F.; Dickey, C. A.; Buratti, E.; Baralle, F.; Bailey, R.; Pickering-Brown, S.; Dickson, D.; Petrucelli, L. Progranulin mediates caspase-dependent cleavage of TAR DNA binding protein-43. *J. Neurosci.* **2007**, *27*, 10530−10534.
(48) Zhang, Y. J.; Xu, Y. F.; Cook, C.; Gendron, T. F.; Roettges, P.; Link, C. D.; Lin, W. L.; Tong, J.; Castanedes-Casey, M.; Ash, P.; Gass, J.; Rangachari, V.; Buratti, E.; Baralle, F.; Golde, T. E.; Dickson, D. W.; Petrucelli, L. Aberrant cleavage of TDP-43 enhances aggregation and cellular toxicity. *Proc. Natl. Acad. Sci. U. S. A.* **2009**, *106*, 7607−12.
(49) Gerstberger, S.; Hafner, M.; Tuschl, T. A census of human RNA-binding proteins. *Nat. Rev. Genet* **2014**, *15*, 829−845.
(50) Marchese, D.; de Groot, N. S.; Lorenzo Gotor, N.; Livi, C. M.; Tartaglia, G. G. Advances in the characterization of RNA-binding proteins. *Wiley Interdiscip Rev. RNA* **2016**, *7*, 793−810.
(51) Conlon, E. G.; Manley, J. L. RNA-binding proteins in neurodegeneration: Mechanisms in aggregate. *Genes Dev.* **2017**, *31*, 1509−1528.
(52) Buratti, E.; Baralle, F. E. Characterization and functional implications of the RNA binding properties of nuclear factor TDP-43, a novel splicing regulator of cftr exon 9. *J. Biol. Chem.* **2001**, *276*, 36337−36343.
(53) Casafont, I.; Bengoechea, R.; Tapia, O.; Berciano, M. T.; Lafarga, M. TDP-43 localizes in mRNA transcription and processing sites in mammalian neurons. *J. Struct Biol.* **2009**, *167*, 235−241.
(54) Tollervey, J. R.; Curk, T.; Rogelj, B.; Briese, M.; Cereda, M.; Kayikci, M.; Konig, J.; Hortobagyi, T.; Nishimura, A. L.; Zupunski, V.; Patani, R.; Chandran, S.; Rot, G.; Zupan, B.; Shaw, C. E.; Ule, J. Characterizing the RNA targets and position-dependent splicing regulation by TDP-43. *Nat. Neurosci.* **2011**, *14*, 452−8.

https://doi.org/10.1021/acsomega.4c04119
ACS Omega 2024, 9, 40286−40297

(55) Maris, C.; Dominguez, C.; Allain, F. H. The RNA recognition motif, a plastic RNA-binding platform to regulate post-transcriptional gene expression. *FEBS J.* **2005**, *272*, 2118−31.
(56) Shodai, A.; Morimura, T.; Ido, A.; Uchida, T.; Ayaki, T.; Takahashi, R.; Kitazawa, S.; Suzuki, S.; Shirouzu, M.; Kigawa, T.; Muto, Y.; Yokoyama, S.; Takahashi, R.; Kitahara, R.; Ito, H.; Fujiwara, N.; Urushitani, M. Aberrant assembly of RNA recognition motif 1 links to pathogenic conversion of TAR DNA-binding protein of 43 kDa (TDP-43). *J. Biol. Chem.* **2013**, *288*, 14886−14905.
(57) Kuo, P. H.; Chiang, C. H.; Wang, Y. T.; Doudeva, L. G.; Yuan, H. S. The crystal structure of TDP-43 RRM1-DNA complex reveals the specific recognition for UG- and TG-rich nucleic acids. *Nucleic Acids Res.* **2014**, *42*, 4712−4722.
(58) Huang, Y. C.; Lin, K. F.; He, R. Y.; Tu, P. H.; Koubek, J.; Hsu, Y. C.; Huang, J. J. Inhibition of TDP-43 aggregation by nucleic acid binding. *PLoS One* **2013**, *8*, No. e64002.
(59) Sun, Y.; Arslan, P. E.; Won, A.; Yip, C. M.; Chakrabartty, A. Binding of TDP-43 to the 3′utr of its cognate mRNA enhances its solubility. *Biochemistry* **2014**, *53*, 5885−94.
(60) Zacco, E.; Grana-Montes, R.; Martin, S. R.; de Groot, N. S.; Alfano, C.; Tartaglia, G. G.; Pastore, A. RNA as a key factor in driving or preventing self-assembly of the TAR DNA-binding protein 43. *J. Mol. Biol.* **2019**, *431*, 1671−1688.
(61) Shenoy, J.; El Mammeri, N.; Dutour, A.; Berbon, M.; Saad, A.; Lends, A.; Morvan, E.; Grelard, A.; Lecomte, S.; Kauffmann, B.; Theillet, F. X.; Habenstein, B.; Loquet, A. Structural dissection of amyloid aggregates of TDP-43 and its C-terminal fragments TDP-35 and TDP-16. *FEBS J.* **2020**, *287*, 2449−2467.
(62) Zacco, E.; Martin, S. R.; Thorogate, R.; Pastore, A. The RNA-recognition motifs of TAR DNA-binding protein 43 may play a role in the aberrant self-assembly of the protein. *Front. Mol. Neurosci.* **2018**, *11*, No. 372.
(63) Pillai, M.; Jha, S. K. The folding and aggregation energy landscapes of tethered RRM domains of human TDP-43 are coupled via a metastable molten globule-like oligomer. *Biochemistry* **2019**, *58*, 608−620.
(64) Pillai, M.; Jha, S. K. Early metastable assembly during the stress-induced formation of worm-like amyloid fibrils of nucleic acid binding domains of TDP-43. *Biochemistry* **2020**, *59*, 315−328.
(65) Shodai, A.; Ido, A.; Fujiwara, N.; Ayaki, T.; Morimura, T.; Oono, M.; Uchida, T.; Takahashi, R.; Ito, H.; Urushitani, M. Conserved acidic amino acid residues in a second RNA recognition motif regulate assembly and function of TDP-43. *PLoS One* **2012**, *7*, No. e52776.
(66) Patni, D.; Jha, S. K. Protonation-deprotonation switch controls the amyloid-like misfolding of nucleic-acid-binding domains of TDP-43. *J. Phys. Chem. B* **2021**, *125*, 8383−8394.
(67) Pillai, M.; Jha, S. K. Multistep molecular mechanism of amyloid-like aggregation of nucleic acid-binding domain of TDP-43. *Proteins* **2023**, *91*, 649−664.
(68) Pillai, M.; Das, A.; Jha, S. K. Electrostatic modulation of intramolecular and intermolecular interactions during the formation of an amyloid-like assembly. *Biochemistry* **2023**, *62*, 1890−1905.
(69) Doke, A. A.; Jha, S. K. Effect of in vitro solvation conditions on inter- and intramolecular assembly of full-length TDP-43. *J. Phys. Chem. B* **2022**, *126*, 4799−4813.
(70) Singh, J.; Udgaonkar, J. B. Unraveling the molecular mechanism of pH-induced misfolding and oligomerization of the prion protein. *J. Mol. Biol.* **2016**, *428*, 1345−1355.
(71) Colon, W.; Kelly, J. W. Partial denaturation of transthyretin is sufficient for amyloid fibril formation in vitro. *Biochemistry* **1992**, *31*, 8654−8660.
(72) Pasquato, N.; Berni, R.; Folli, C.; Alfieri, B.; Cendron, L.; Zanotti, G. Acidic pH-induced conformational changes in amyloidogenic mutant transthyretin. *J. Mol. Biol.* **2007**, *366*, 711−9.
(73) Khurana, R.; Gillespie, J. R.; Talapatra, A.; Minert, L. J.; Ionescu-Zanetti, C.; Millett, I.; Fink, A. L. Partially folded intermediates as critical precursors of light chain amyloid fibrils and amorphous aggregates. *Biochemistry* **2001**, *40*, 3525−3535.
(74) Hornemann, S.; Glockshuber, R. A scrapie-like unfolding intermediate of the prion protein domain prp(121−231) induced by acidic pH. *Proc. Natl. Acad. Sci. U. S. A.* **1998**, *95*, 6010−6014.
(75) Peralvarez-Marin, A.; Barth, A.; Graslund, A. Time-resolved infrared spectroscopy of pH-induced aggregation of the Alzheimer abeta(1−28) peptide. *J. Mol. Biol.* **2008**, *379*, 589−96.
(76) McParland, V. J.; Kad, N. M.; Kalverda, A. P.; Brown, A.; Kirwin-Jones, P.; Hunter, M. G.; Sunde, M.; Radford, S. E. Partially unfolded states of beta(2)-microglobulin and amyloid formation in vitro. *Biochemistry* **2000**, *39*, 8735−46.
(77) Rabouille, C.; Alberti, S. Cell adaptation upon stress: The emerging role of membrane-less compartments. *Curr. Opin. Cell Biol.* **2017**, *47*, 34−42.
(78) Skora, L.; Becker, S.; Zweckstetter, M. Molten globule precursor states are conformationally correlated to amyloid fibrils of human beta-2-microglobulin. *J. Am. Chem. Soc.* **2010**, *132*, 9223−5.
(79) Carrotta, R.; Bauer, R.; Waninge, R.; Rischel, C. Conformational characterization of oligomeric intermediates and aggregates in beta-lactoglobulin heat aggregation. *Protein Sci.* **2001**, *10*, 1312−1318.
(80) Honda, R. P.; Yamaguchi, K. I.; Kuwata, K. Acid-induced molten globule state of a prion protein: Crucial role of strand 1-helix 1-strand 2 segment. *J. Biol. Chem.* **2014**, *289*, 30355−30363.
(81) Ano Bom, A. P. D.; Freitas, M. S.; Moreira, F. S.; Ferraz, D.; Sanches, D.; Gomes, A. M.O.; Valente, A. P.; Cordeiro, Y.; Silva, J. L. The p53 core domain is a molten globule at low pH: Functional implications of a partially unfolded structure. *J. Biol. Chem.* **2010**, *285*, 2857−2866.
(82) Pedrote, M. M.; de Oliveira, G. A. P.; Felix, A. L.; Mota, M. F.; Marques, M. A.; Soares, I. N.; Iqbal, A.; Norberto, D. R.; Gomes, A. M. O.; Gratton, E.; Cino, E. A.; Silva, J. L. Aggregation-primed molten globule conformers of the p53 core domain provide potential tools for studying p53c aggregation in cancer. *J. Biol. Chem.* **2018**, *293*, 11374−11387.
(83) Austin, J. A.; Wright, G. S. A.; Watanabe, S.; Grossmann, J. G.; Antonyuk, S. V.; Yamanaka, K.; Hasnain, S. S. Disease causing mutants of TDP-43 nucleic acid binding domains are resistant to aggregation and have increased stability and half-life. *Proc. Natl. Acad. Sci. U. S. A.* **2014**, *111*, 4309−4314.
(84) Moreno, F.; Rabinovici, G. D.; Karydas, A.; Miller, Z.; Hsu, S. C.; Legati, A.; Fong, J.; Schonhaut, D.; Esselmann, H.; Watson, C.; Stephens, M. L.; Kramer, J.; Wiltfang, J.; Seeley, W. W.; Miller, B. L.; Coppola, G.; Grinberg, L. T. A novel mutation P112H in the TARDBP gene associated with frontotemporal lobar degeneration without motor neuron disease and abundant neuritic amyloid plaques. *Acta Neuropathol. Commun.* **2015**, *3*, No. 19.
(85) Chiang, C. H.; Grauffel, C.; Wu, L. S.; Kuo, P. H.; Doudeva, L. G.; Lim, C.; Shen, C. K.; Yuan, H. S. Structural analysis of disease-related TDP-43 D169G mutation: Linking enhanced stability and caspase cleavage efficiency to protein accumulation. *Sci. Rep.* **2016**, *6*, 21581.
(86) Chang, C. K.; Chiang, M. H.; Toh, E. K.; Chang, C. F.; Huang, T. H. Molecular mechanism of oxidation-induced TDP-43 RRM1 aggregation and loss of function. *FEBS Lett.* **2013**, *587*, 575−582.
(87) Rabdano, S. O.; Izmailov, S. A.; Luzik, D. A.; Groves, A.; Podkorytov, I. S.; Skrynnikov, N. R. Onset of disorder and protein aggregation due to oxidation-induced intermolecular disulfide bonds: Case study of RRM2 domain from TDP-43. *Sci. Rep.* **2017**, *7*, 11161.
(88) Garnier, C.; Devred, F.; Byrne, D.; Puppo, R.; Roman, A. Y.; Malesinski, S.; Golovin, A. V.; Lebrun, R.; Ninkina, N. N.; Tsvetkov, P. O. Zinc binding to RNA recognition motif of TDP-43 induces the formation of amyloid-like aggregates. *Sci. Rep.* **2017**, *7*, 6812.
(89) Mackness, B. C.; Tran, M. T.; McClain, S. P.; Matthews, C. R.; Zitzewitz, J. A. Folding of the RNA recognition motif (RRM) domains of the amyotrophic lateral sclerosis (ALS)-linked protein TDP-43 reveals an intermediate state. *J. Biol. Chem.* **2014**, *289*, 8264−8276.
(90) Lukong, K. E.; Chang, K. W.; Khandjian, E. W.; Richard, S. RNA-binding proteins in human genetic disease. *Trends Genet* **2008**, *24*, 416−425.

https://doi.org/10.1021/acsomega.4c04119
ACS Omega 2024, 9, 40286−40297

(91) Harrison, A. F.; Shorter, J. RNA-binding proteins with prion-like domains in health and disease. *Biochem. J.* **2017**, *474*, 1417−1438.
(92) Agrawal, S.; Kuo, P. H.; Chu, L. Y.; Golzarroshan, B.; Jain, M.; Yuan, H. S. RNA recognition motifs of disease-linked RNA-binding proteins contribute to amyloid formation. *Sci. Rep.* **2019**, *9*, 6171.
(93) Cascella, R.; Capitini, C.; Fani, G.; Dobson, C. M.; Cecchi, C.; Chiti, F. Quantification of the relative contributions of loss-of-function and gain-of-function mechanisms in TAR DNA-binding protein 43 (TDP-43) proteinopathies. *J. Biol. Chem.* **2016**, *291*, 19437−19448.
(94) Halliday, G.; Bigio, E. H.; Cairns, N. J.; Neumann, M.; Mackenzie, I. R.; Mann, D. M. Mechanisms of disease in frontotemporal lobar degeneration: Gain of function versus loss of function effects. *Acta Neuropathol.* **2012**, *124*, 373−82.
(95) Fang, Y. S.; Tsai, K. J.; Chang, Y. J.; Kao, P.; Woods, R.; Kuo, P. H.; Wu, C. C.; Liao, J. Y.; Chou, S. C.; Lin, V.; Jin, L. W.; Yuan, H. S.; Cheng, I. H.; Tu, P. H.; Chen, Y. R. Full-length TDP-43 forms toxic amyloid oligomers that are present in frontotemporal lobar dementia-TDP patients. *Nat. Commun.* **2014**, *5*, No. 4824.
(96) Kayed, R.; Head, E.; Thompson, J. L.; McIntire, T. M.; Milton, S. C.; Cotman, C. W.; Glabe, C. G. Common structure of soluble amyloid oligomers implies common mechanism of pathogenesis. *Science* **2003**, *300*, 486−489.
(97) Gasset-Rosa, F.; Lu, S.; Yu, H.; Chen, C.; Melamed, Z.; Guo, L.; Shorter, J.; Da Cruz, S.; Cleveland, D. W. Cytoplasmic TDP-43 de-mixing independent of stress granules drives inhibition of nuclear import, loss of nuclear TDP-43, and cell death. *Neuron* **2019**, *102*, No. 339.
(98) Kao, P. F.; Chen, Y. R.; Liu, X. B.; DeCarli, C.; Seeley, W. W.; Jin, L. W. Detection of TDP-43 oligomers in frontotemporal lobar degeneration-TDP. *Ann. Neurol.* **2015**, *78*, 211−221.
(99) Smethurst, P.; Risse, E.; Tyzack, G. E.; Mitchell, J. S.; Taha, D. M.; Chen, Y. R.; Newcombe, J.; Collinge, J.; Sidle, K.; Patani, R. Distinct responses of neurons and astrocytes to TDP-43 proteinopathy in amyotrophic lateral sclerosis. *Brain* **2020**, *143*, 430−440.
(100) Wang, C.; Duan, Y.; Duan, G.; Wang, Q.; Zhang, K.; Deng, X.; Qian, B.; Gu, J.; Ma, Z.; Zhang, S.; Guo, L.; Liu, C.; Fang, Y. Stress induces dynamic, cytotoxicity-antagonizing TDP-43 nuclear bodies via paraspeckle lncrna neat1-mediated liquid-liquid phase separation. *Mol. Cell* **2020**, *79*, No. 443.
(101) Yu, H.; Lu, S.; Gasior, K.; Singh, D.; Vazquez-Sanchez, S.; Tapia, O.; Toprani, D.; Beccari, M. S.; Yates, J. R.; Da Cruz, S.; Newby, J. M.; Lafarga, M.; Gladfelter, A. S.; Villa, E.; Cleveland, D. W. Hsp70 chaperones RNA-free TDP-43 into anisotropic intranuclear liquid spherical shells. *Science* **2021**, *371*, eabb4309.
(102) Keating, S. S.; Bademosi, A. T.; San Gil, R.; Walker, A. K. Aggregation-prone TDP-43 sequesters and drives pathological transitions of free nuclear TDP-43. *Cell. Mol. Life Sci.* **2023**, *80*, 95.
(103) Staderini, T.; Bigi, A.; Mongiello, D.; Cecchi, C.; Chiti, F. Biophysical characterization of full-length TAR DNA-binding protein (TDP-43) phase separation. *Protein Sci.* **2022**, *31*, No. e4509.
(104) Li, H. R.; Chen, T. C.; Hsiao, C. L.; Shi, L.; Chou, C. Y.; Huang, J. R. The physical forces mediating self-association and phase-separation in the C-terminal domain of TDP-43. *Biochim. Biophys. Acta Proteins Proteom.* **2018**, *1866*, 214−223.
(105) Babinchak, W. M.; Haider, R.; Dumm, B. K.; Sarkar, P.; Surewicz, K.; Choi, J. K.; Surewicz, W. K. The role of liquid-liquid phase separation in aggregation of the TDP-43 low-complexity domain. *J. Biol. Chem.* **2019**, *294*, 6306−6317.
(106) Mackenzie, I. R.; Nicholson, A. M.; Sarkar, M.; Messing, J.; Purice, M. D.; Pottier, C.; Annu, K.; Baker, M.; Perkerson, R. B.; Kurti, A.; Matchett, B. J.; Mittag, T.; Temirov, J.; Hsiung, G. R.; Krieger, C.; Murray, M. E.; Kato, M.; Fryer, J. D.; Petrucelli, L.; Zinman, L.; Weintraub, S.; Mesulam, M.; Keith, J.; Zivkovic, S. A.; Hirsch-Reinshagen, V.; Roos, R. P.; Zuchner, S.; Graff-Radford, N. R.; Petersen, R. C.; Caselli, R. J.; Wszolek, Z. K.; Finger, E.; Lippa, C.; Lacomis, D.; Stewart, H.; Dickson, D. W.; Kim, H. J.; Rogaeva, E.; Bigio, E.; Boylan, K. B.; Taylor, J. P.; Rademakers, R. Tia1 mutations in amyotrophic lateral sclerosis and frontotemporal dementia promote phase separation and alter stress granule dynamics. *Neuron* **2017**, *95*, 808−816.
(107) Kim, H. J.; Kim, N. C.; Wang, Y. D.; Scarborough, E. A.; Moore, J.; Diaz, Z.; MacLea, K. S.; Freibaum, B.; Li, S.; Molliex, A.; Kanagaraj, A. P.; Carter, R.; Boylan, K. B.; Wojtas, A. M.; Rademakers, R.; Pinkus, J. L.; Greenberg, S. A.; Trojanowski, J. Q.; Traynor, B. J.; Smith, B. N.; Topp, S.; Gkazi, A. S.; Miller, J.; Shaw, C. E.; Kottlors, M.; Kirschner, J.; Pestronk, A.; Li, Y. R.; Ford, A. F.; Gitler, A. D.; Benatar, M.; King, O. D.; Kimonis, V. E.; Ross, E. D.; Weihl, C. C.; Shorter, J.; Taylor, J. P. Mutations in prion-like domains in hnrnpa2b1 and hnrnpa1 cause multisystem proteinopathy and ALS. *Nature* **2013**, *495*, 467−473.
(108) Panas, M. D.; Ivanov, P.; Anderson, P. Mechanistic insights into mammalian stress granule dynamics. *J. Cell Biol.* **2016**, *215*, 313−323.
(109) Jain, S.; Wheeler, J. R.; Walters, R. W.; Agrawal, A.; Barsic, A.; Parker, R. Atpase-modulated stress granules contain a diverse proteome and substructure. *Cell* **2016**, *164*, 487−498.
(110) Volkening, K.; Leystra-Lantz, C.; Yang, W. C.; Jaffee, H.; Strong, M. J. Tar DNA binding protein of 43 kDa (TDP-43), 14−3-3 proteins and copper/zinc superoxide dismutase (SOD1) interact to modulate NFL mRNA stability. Implications for altered RNA processing in amyotrophic lateral sclerosis (ALS). *Brain Res.* **2009**, *1305*, 168−182.
(111) Dormann, D.; Rodde, R.; Edbauer, D.; Bentmann, E.; Fischer, I.; Hruscha, A.; Than, M. E.; Mackenzie, I. R.; Capell, A.; Schmid, B.; Neumann, M.; Haass, C. ALS-associated fused in sarcoma (FUS) mutations disrupt transportin-mediated nuclear import. *EMBO J.* **2010**, *29*, 2841−57.
(112) Liu-Yesucevitz, L.; Bilgutay, A.; Zhang, Y. J.; Vanderwyde, T.; Citro, A.; Mehta, T.; Zaarur, N.; McKee, A.; Bowser, R.; Sherman, M.; Petrucelli, L.; Wolozin, B. Tar DNA binding protein-43 (TDP-43) associates with stress granules: Analysis of cultured cells and pathological brain tissue. *PLoS One* **2010**, *5*, No. e13250.
(113) Bentmann, E.; Neumann, M.; Tahirovic, S.; Rodde, R.; Dormann, D.; Haass, C. Requirements for stress granule recruitment of fused in sarcoma (FUS) and TAR DNA-binding protein of 43 kDa (TDP-43). *J. Biol. Chem.* **2012**, *287*, 23079−23094.
(114) McGurk, L.; Lee, V. M.; Trojanowksi, J. Q.; Van Deerlin, V. M.; Lee, E. B.; Bonini, N. M. Poly-a binding protein-1 localization to a subset of TDP-43 inclusions in amyotrophic lateral sclerosis occurs more frequently in patients harboring an expansion in c9orf72. *J. Neuropathol Exp Neurol* **2014**, *73*, 837−45.
(115) Mori, F.; Yasui, H.; Miki, Y.; Kon, T.; Arai, A.; Kurotaki, H.; Tomiyama, M.; Wakabayashi, K. Colocalization of TDP-43 and stress granules at the early stage of TDP-43 aggregation in amyotrophic lateral sclerosis. *Brain Pathol* **2024**, *34*, No. e13215.
(116) Bentmann, E.; Haass, C.; Dormann, D. Stress granules in neurodegeneration–lessons learnt from TAR DNA binding protein of 43 kDa and fused in sarcoma. *FEBS J.* **2013**, *280*, 4348−4370.
(117) Wolozin, B. The evolution of phase-separated TDP-43 in stress. *Neuron* **2019**, *102*, 265−267.
(118) Nonaka, T.; Masuda-Suzukake, M.; Arai, T.; Hasegawa, Y.; Akatsu, H.; Obi, T.; Yoshida, M.; Murayama, S.; Mann, D. M. A.; Akiyama, H.; Hasegawa, M. Prion-like properties of pathological TDP-43 aggregates from diseased brains. *Cell Rep* **2013**, *4*, 124−134.
(119) Hasegawa, M.; Arai, T.; Nonaka, T.; Kametani, F.; Yoshida, M.; Hashizume, Y.; Beach, T. G.; Buratti, E.; Baralle, F.; Morita, M.; Nakano, I.; Oda, T.; Tsuchiya, K.; Akiyama, H. Phosphorylated TDP-43 in frontotemporal lobar degeneration and amyotrophic lateral sclerosis. *Ann. Neurol.* **2008**, *64*, 60−70.
(120) Lin, W. L.; Dickson, D. W. Ultrastructural localization of TDP-43 in filamentous neuronal inclusions in various neurodegenerative diseases. *Acta Neuropathol.* **2008**, *116*, 205−13.
(121) Mori, F.; Tanji, K.; Zhang, H. X.; Nishihira, Y.; Tan, C. F.; Takahashi, H.; Wakabayashi, K. Maturation process of TDP-43-positive neuronal cytoplasmic inclusions in amyotrophic lateral sclerosis with and without dementia. *Acta Neuropathol.* **2008**, *116*, 193−203.

https://doi.org/10.1021/acsomega.4c04119
ACS Omega 2024, 9, 40286−40297

(122) Arseni, D.; Hasegawa, M.; Murzin, A. G.; Kametani, F.; Arai, M.; Yoshida, M.; Ryskeldi-Falcon, B. Structure of pathological TDP-43 filaments from ALS with ftld. *Nature* **2022**, *601*, 139−143.
(123) Cao, Q.; Boyer, D. R.; Sawaya, M. R.; Ge, P.; Eisenberg, D. S. Cryo-em structures of four polymorphic TDP-43 amyloid cores. *Nat. Struct. Mol. Biol.* **2019**, *26*, 619−627.
(124) Li, Q.; Babinchak, W. M.; Surewicz, W. K. Cryo-em structure of amyloid fibrils formed by the entire low complexity domain of TDP-43. *Nat. Commun.* **2021**, *12*, 1620.
(125) Arseni, D.; Chen, R.; Murzin, A. G.; Peak-Chew, S. Y.; Garringer, H. J.; Newell, K. L.; Kametani, F.; Robinson, A. C.; Vidal, R.; Ghetti, B.; Hasegawa, M.; Ryskeldi-Falcon, B. TDP-43 forms amyloid filaments with a distinct fold in type a ftld-TDP. *Nature* **2023**, *620*, 898−903.
(126) Close, W.; Neumann, M.; Schmidt, A.; Hora, M.; Annamalai, K.; Schmidt, M.; Reif, B.; Schmidt, V.; Grigorieff, N.; Fandrich, M. Physical basis of amyloid fibril polymorphism. *Nat. Commun.* **2018**, *9*, 699.
(127) Almeida, Z. L.; Brito, R. M. M. Structure and aggregation mechanisms in amyloids. *Molecules* **2020**, *25*, 1195.
(128) Chiti, F.; Dobson, C. M. Protein misfolding, amyloid formation, and human disease: A summary of progress over the last decade. *Annu. Rev. Biochem.* **2017**, *86*, 27−68.
(129) Petkova, A. T.; Leapman, R. D.; Guo, Z.; Yau, W. M.; Mattson, M. P.; Tycko, R. Self-propagating, molecular-level polymorphism in alzheimer's beta-amyloid fibrils. *Science* **2005**, *307*, 262−5.
(130) Bertini, I.; Gonnelli, L.; Luchinat, C.; Mao, J.; Nesi, A. A new structural model of abeta40 fibrils. *J. Am. Chem. Soc.* **2011**, *133*, 16013−16022.
(131) Niu, Z.; Zhao, W.; Zhang, Z.; Xiao, F.; Tang, X.; Yang, J. The molecular structure of Alzheimer beta-amyloid fibrils formed in the presence of phospholipid vesicles. *Angew. Chem.* **2014**, *53*, 9294−7.
(132) Meinhardt, J.; Sachse, C.; Hortschansky, P.; Grigorieff, N.; Fandrich, M. Abeta(1−40) fibril polymorphism implies diverse interaction patterns in amyloid fibrils. *J. Mol. Biol.* **2009**, *386*, 869−77.
(133) Lu, J. X.; Qiang, W.; Yau, W. M.; Schwieters, C. D.; Meredith, S. C.; Tycko, R. Molecular structure of beta-amyloid fibrils in alzheimer's disease brain tissue. *Cell* **2013**, *154*, 1257−1268.
(134) Bousset, L.; Pieri, L.; Ruiz-Arlandis, G.; Gath, J.; Jensen, P. H.; Habenstein, B.; Madiona, K.; Olieric, V.; Bockmann, A.; Meier, B. H.; Melki, R. Structural and functional characterization of two alpha-synuclein strains. *Nat. Commun.* **2013**, *4*, 2575.
(135) Heise, H.; Hoyer, W.; Becker, S.; Andronesi, O. C.; Riedel, D.; Baldus, M. Molecular-level secondary structure, polymorphism, and dynamics of full-length alpha-synuclein fibrils studied by solid-state NMR. *Proc. Natl. Acad. Sci. U. S. A.* **2005**, *102*, 15871−15876.
(136) Lemkau, L. R.; Comellas, G.; Kloepper, K. D.; Woods, W. S.; George, J. M.; Rienstra, C. M. Mutant protein a30p alpha-synuclein adopts wild-type fibril structure, despite slower fibrillation kinetics. *J. Biol. Chem.* **2012**, *287*, 11526−11532.
(137) Luca, S.; Yau, W. M.; Leapman, R.; Tycko, R. Peptide conformation and supramolecular organization in amylin fibrils: Constraints from solid-state NMR. *Biochemistry* **2007**, *46*, 13505−13522.
(138) Andronesi, O. C.; von Bergen, M.; Biernat, J.; Seidel, K.; Griesinger, C.; Mandelkow, E.; Baldus, M. Characterization of alzheimer's-like paired helical filaments from the core domain of tau protein using solid-state NMR spectroscopy. *J. Am. Chem. Soc.* **2008**, *130*, 5922−5928.
(139) Daebel, V.; Chinnathambi, S.; Biernat, J.; Schwalbe, M.; Habenstein, B.; Loquet, A.; Akoury, E.; Tepper, K.; Muller, H.; Baldus, M.; Griesinger, C.; Zweckstetter, M.; Mandelkow, E.; Vijayan, V.; Lange, A. Beta-sheet core of tau paired helical filaments revealed by solid-state NMR. *J. Am. Chem. Soc.* **2012**, *134*, 13982−13989.
(140) Theint, T.; Nadaud, P. S.; Aucoin, D.; Helmus, J. J.; Pondaven, S. P.; Surewicz, K.; Surewicz, W. K.; Jaroniec, C. P. Species-dependent structural polymorphism of y145stop prion protein amyloid revealed by solid-state NMR spectroscopy. *Nat. Commun.* **2017**, *8*, 753.
(141) DePace, A. H.; Weissman, J. S. Origins and kinetic consequences of diversity in sup35 yeast prion fibers. *Nat. Struct. Biol.* **2002**, *9*, 389−396.
(142) Tanaka, M.; Chien, P.; Naber, N.; Cooke, R.; Weissman, J. S. Conformational variations in an infectious protein determine prion strain differences. *Nature* **2004**, *428*, 323−8.
(143) Wolynes, P. G.; Onuchic, J. N.; Thirumalai, D. Navigating the folding routes. *Science* **1995**, *267*, 1619−20.
(144) Dill, K. A.; Chan, H. S. From levinthal to pathways to funnels. *Nat. Struct. Biol.* **1997**, *4*, 10−9.
(145) Gershenson, A.; Gierasch, L. M.; Pastore, A.; Radford, S. E. Energy landscapes of functional proteins are inherently risky. *Nat. Chem. Biol.* **2014**, *10*, 884−891.
(146) Dobson, C. M. Protein misfolding, evolution and disease. *Trends Biochem. Sci.* **1999**, *24*, 329−332.
(147) Uversky, V. N.; Fink, A. L. Conformational constraints for amyloid fibrillation: The importance of being unfolded. *Biochim. Biophys. Acta* **2004**, *1698*, 131−53.
(148) Lansbury, P. T., Jr. Evolution of amyloid: What normal protein folding may tell us about fibrillogenesis and disease. *Proc. Natl. Acad. Sci. U. S. A.* **1999**, *96*, 3342−3344.
(149) Fink, A. L. Protein aggregation: Folding aggregates, inclusion bodies and amyloid. *Fold Des* **1998**, *3*, R9−23.
(150) Zerovnik, E. Amyloid-fibril formation. Proposed mechanisms and relevance to conformational disease. *Eur. J. Biochem.* **2002**, *269*, 3362−3371.
(151) Jain, S.; Udgaonkar, J. B. Evidence for stepwise formation of amyloid fibrils by the mouse prion protein. *J. Mol. Biol.* **2008**, *382*, 1228−1241.
(152) Moulick, R.; Das, R.; Udgaonkar, J. B. Partially unfolded forms of the prion protein populated under misfolding-promoting conditions: Characterization by hydrogen exchange mass spectrometry and NMR. *J. Biol. Chem.* **2015**, *290*, 25227−40.
(153) Niu, B.; Mackness, B. C.; Zitzewitz, J. A.; Matthews, C. R.; Gross, M. L. Trifluoroethanol partially unfolds g93a SOD1 leading to protein aggregation: A study by native mass spectrometry and fpop protein footprinting. *Biochemistry* **2020**, *59*, 3650−3659.
(154) Quintas, A.; Vaz, D. C.; Cardoso, I.; Saraiva, M. J.; Brito, R. M. Tetramer dissociation and monomer partial unfolding precedes protofibril formation in amyloidogenic transthyretin variants. *J. Biol. Chem.* **2001**, *276*, 27207−13.
(155) Bulawa, C. E.; Connelly, S.; Devit, M.; Wang, L.; Weigel, C.; Fleming, J. A.; Packman, J.; Powers, E. T.; Wiseman, R. L.; Foss, T. R.; Wilson, I. A.; Kelly, J. W.; Labaudiniere, R. Tafamidis, a potent and selective transthyretin kinetic stabilizer that inhibits the amyloid cascade. *Proc. Natl. Acad. Sci. U. S. A.* **2012**, *109*, 9629−9634.
(156) Yan, N. L.; Santos-Martins, D.; Rennella, E.; Sanchez, B. B.; Chen, J. S.; Kay, L. E.; Wilson, I. A.; Morgan, G. J.; Forli, S.; Kelly, J. W. Structural basis for the stabilization of amyloidogenic immunoglobulin light chains by hydantoins. *Bioorg. Med. Chem. Lett.* **2020**, *30*, 127356.
(157) Yang, L.; Jasiqi, Y.; Zettor, A.; Vadas, O.; Chiaravalli, J.; Agou, F.; Lashuel, H. A. Effective inhibition of TDP-43 aggregation by native state stabilization. *Angew. Chem.* **2024**, *63*, No. e202314587.
(158) Cawood, E. E.; Guthertz, N.; Ebo, J. S.; Karamanos, T. K.; Radford, S. E.; Wilson, A. J. Modulation of amyloidogenic protein self-assembly using tethered small molecules. *J. Am. Chem. Soc.* **2020**, *142*, 20845−20854.
(159) Chang, H. Y.; Wang, I. F. Restoring functional TDP-43 oligomers in ALS and laminopathic cellular models through baicalein-induced reconfiguration of TDP-43 aggregates. *Sci. Rep.* **2024**, *14*, 4620.
(160) Rui, W.; Li, S.; Xiao, H.; Xiao, M.; Shi, J. Baicalein attenuates neuroinflammation by inhibiting nlrp3/caspase-1/gsdmd pathway in mptp induced mice model of parkinson's disease. *Int. J. Neuropsychopharmacol* **2020**, *23*, 762−73.

https://doi.org/10.1021/acsomega.4c04119
ACS Omega 2024, 9, 40286−40297

(161) Murray, K. A.; Hu, C. J.; Griner, S. L.; Pan, H.; Bowler, J. T.; Abskharon, R.; Rosenberg, G. M.; Cheng, X.; Seidler, P. M.; Eisenberg, D. S. De novo designed protein inhibitors of amyloid aggregation and seeding. *Proc. Natl. Acad. Sci. U. S. A.* **2022**, *119*, No. e2206240119.
(162) Kochen, N. N.; Vasandani, V.; Seaney, D.; Pandey, A. K.; Walters, M. A.; Braun, A. R.; Sachs, J. N. Threonine cavities are targetable motifs that control alpha-synuclein fibril growth. *ACS Chem. Neurosci.* **2022**, *13*, 2646−2657.
(163) Antonschmidt, L.; Matthes, D.; Dervisoglu, R.; Frieg, B.; Dienemann, C.; Leonov, A.; Nimerovsky, E.; Sant, V.; Ryazanov, S.; Giese, A.; Schroder, G. F.; Becker, S.; de Groot, B. L.; Griesinger, C.; Andreas, L. B. The clinical drug candidate anle138b binds in a cavity of lipidic alpha-synuclein fibrils. *Nat. Commun.* **2022**, *13*, 5385.
(164) Spanopoulou, A.; Heidrich, L.; Chen, H. R.; Frost, C.; Hrle, D.; Malideli, E.; Hille, K.; Grammatikopoulos, A.; Bernhagen, J.; Zacharias, M.; Rammes, G.; Kapurniotu, A. Designed macrocyclic peptides as nanomolar amyloid inhibitors based on minimal recognition elements. *Angew. Chem.* **2018**, *57*, 14503−14508.
(165) Tas, K.; Dalla Volta, B.; Lindner, C.; El Bounkari, O.; Hille, K.; Tian, Y.; Puig-Bosch, X.; Ballmann, M.; Hornung, S.; Ortner, M.; Prem, S.; Meier, L.; Rammes, G.; Haslbeck, M.; Weber, C.; Megens, R. T. A.; Bernhagen, J.; Kapurniotu, A. Designed peptides as nanomolar cross-amyloid inhibitors acting via supramolecular nanofiber co-assembly. *Nat. Commun.* **2022**, *13*, 5004.
(166) Michaels, T. C. T.; Saric, A.; Meisl, G.; Heller, G. T.; Curk, S.; Arosio, P.; Linse, S.; Dobson, C. M.; Vendruscolo, M.; Knowles, T. P. J. Thermodynamic and kinetic design principles for amyloid-aggregation inhibitors. *Proc. Natl. Acad. Sci. U. S. A.* **2020**, *117*, 24251−24257.

https://doi.org/10.1021/acsomega.4c04119
ACS Omega 2024, 9, 40286−40297